Progress In Electromagnetics Research, Vol. 153, 113–121, 2015

Ultrashort Microwave Pulse Generation by Passive Pulse Compression in a Compact Reverberant Cavity

Sun K. Hong[1, *], Emily Lathrop[2], Victor M. Mendez[1], and Jerry Kim[1]

Abstract—In this paper, we demonstrate a device that is capable of generating an ultrashort (sub-nanosecond) high power microwave pulse by means of passive pulse compression in a compact reverberant cavity. The long duration input pulse into the cavity is created using time-reversal techniques, which allows the waveform to contain the inverse profile of the cavity phase distortion. When fed back into the cavity, the wave focusing at the output port results in a compressed ultrashort pulse with enhanced peak amplitude. We experimentally demonstrate a pulse compressor consisting of a 0.0074 m^3 cavity capable of generating a 130 picosecond pulse from an input waveform of 300 nanosecond duration with the peak gain of up to 19 dB.

1. INTRODUCTION

Microwave pulse compression is a technique for converting a long duration, low amplitude pulse into a short, high peak pulse. The benefit of pulse compression is that it allows for significantly higher peak power to be generated from a source whose output peak power is otherwise limited. For this reason, pulse compression has been of interest for various applications such as particle accelerators, radars and directed energy [1, 2].

Historically, pulse compression can be achieved either actively or passively. An active pulse compressor consists of a resonant cavity with an embedded switch where narrowband microwave energy is stored in the cavity until the switch is tuned on to generate a sudden shift in the eigenmodes, temporarily destroying the cavity Q and causing the release of the energy in the form of a short, high power pulse [3–5]. A passive approach is to use a dispersive waveguide structure, where an input pulse containing the inverse dispersion profile is compressed into a short pulse with enhanced peak power as a result of the effective cancelation of dispersion [6–8]. The choice of pulse compression methods depends on the pulsewidth, power level, peak gain and frequencies of interest for a specific application.

There is interest in generating ultrashort, sub-nanosecond pulses that can be utilized in various areas such as directed energy, high resolution radar, wireless power transfer and biomedical applications [9–13]. Pulse compression could significantly increase achievable peak power in generating such pulses. However, the aforementioned pulse compression approaches may not be suitable due to their physical design constraints which limit the bandwidth, rendering these techniques incapable of generating ultrashort microwave pulses. Such a limitation comes from the switching speed and cavity size (for resonant cavity pulse compressors) and the dispersion rate (for dispersive waveguide pulse compressors).

In this paper, we present a passive pulse compressor based on a compact reverberant cavity that is capable of generating ultrashort microwave pulses. By applying time-reversal (TR) techniques, a long duration input pulse is created. As a result of wave focusing at the cavity output due to time-reversal, a compressed short pulse with peak power significantly higher than the input pulse is generated.

Received 24 September 2015, Accepted 30 October 2015, Scheduled 5 November 2015

* Corresponding author: Sun K. Hong (hong@rose-hulman.edu).

[1] Code 5745, Naval Research Laboratory, 4555 Overlook Ave. SW, Washington, DC 20375, USA. [2] Envisioneering, Inc., 5904 Richmond Hwy. Alexandria, VA 22303, USA.

In particular, we utilize one-bit time-reversal (OBTR) [14] to create input waveforms with uniform amplitude. OBTR has been applied to achieve high peak time-reversal reconstruction for various acoustic and electromagnetic applications [14–17]. Fig. 1 presents a schematic diagram of the proposed passive pulse compressor. As shown in the figure, the input waveform is created by recording the impulse response of the same reverberation cavity used as a pulse compressor. The impulse response is then modified to have uniform amplitude by means of OBTR. In the pulse compression stage, the input waveform is fed into the cavity (from an arbitrary waveform generator) through an optional amplifier for higher peak power. The output of the cavity is an ultrashort high peak pulse. We experimentally demonstrate the proposed pulse compression using a compact reverberation cavity ($0.0074\,\mathrm{m}^3$), where a 130 ps short pulse is generated with the peak gain of up to 19 dB from an input waveform of 300 ns duration.

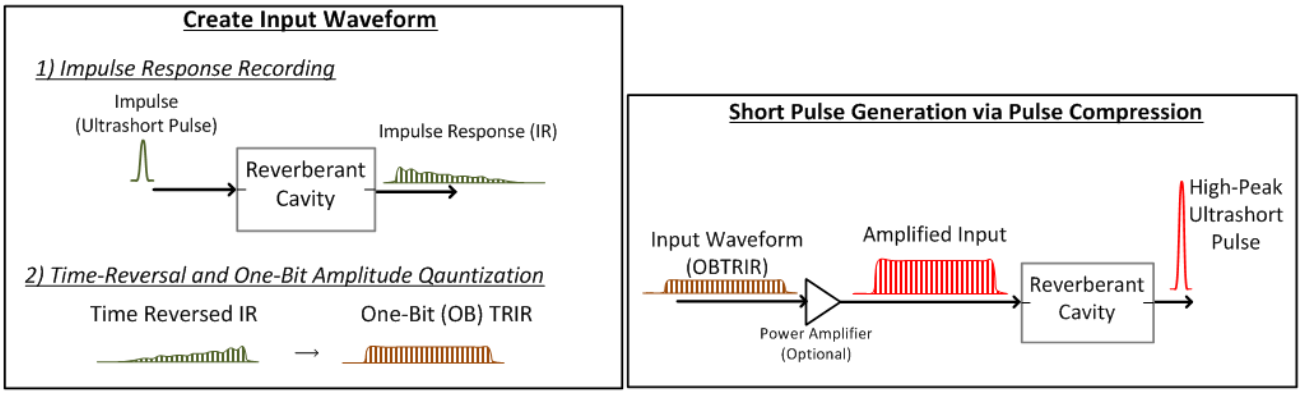

Figure 1. Schematic diagram of the proposed passive pulse compression to generate ultrashort microwave pulses.

The organization of the paper is as follows. In Section 2, the principles of TR and OBTR in a reverberant cavity towards pulse compression are discussed in terms of linear system equations. In Section 3, an experimental demonstration of the proposed pulse compressor is presented. A discussion on the compression gain in relation to cavity eigenmodes and energy efficiency will be presented in Section 4, followed by conclusions in Section 5.

2. REVERBERANT CAVITY AS A PASSIVE PULSE COMPRESSOR

A reverberant cavity provides a complex scattering environment due to the reflecting boundaries from its closed walls and scattering objects placed inside. For an impulse (short pulse) fed into a two-port reverberant cavity, the resulting signal at the output port is a slowly-decaying time-spread response, $h(t)$, representing the sum of a large number of reflected echoes of the impulse over different multipath ray trajectories between the input and output ports. Such a scattering makes the effective propagation length significantly greater than the actual dimensions of the cavity. An example of $h(t)$ is shown in Fig. 2(a), where an impulse of 7 GHz bandwidth (between 2–9 GHz), which corresponds to $\sim$ 130 ps of pulsewidth, was transmitted into a cavity with the dimensions of $0.58 \times 0.32 \times 0.04\,\mathrm{m}^3$ (see Fig. 9. Experiment detail will be discussed in the subsequent section). The amplitude of $h(t)$ is scaled to correspond to the impulse with the magnitude of 1 in the frequency domain (the actual peak amplitude of the original impulse is 0.25 V). In the frequency domain, $h(t)$ is represented by a transfer function $H(\omega)$ (Fig. 2(b)) consisting of closely spaced eigenmodes with random phase distortion. This phase distortion is heavily dependent on the position of the ports and scatterers which determine the propagation condition. In this regard, a reverberant cavity can be viewed as a highly dispersive structure with a random phase response.

The effects of this random dispersion in a reverberant cavity can be "undone" to reconstruct a short pulse by utilizing time-reversal (TR) [18, 19]. This is done by transmitting a time-reversed version

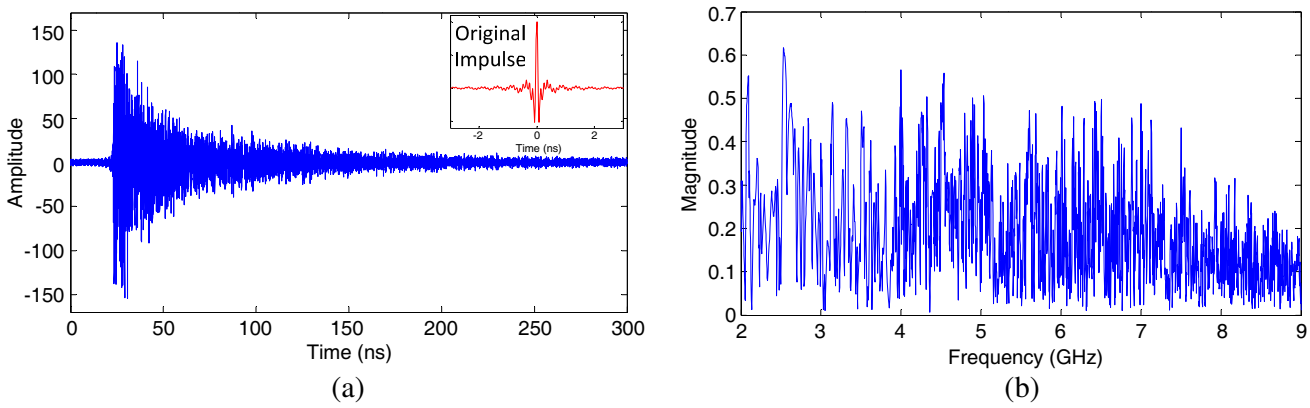

Figure 2. The impulse response and the corresponding transfer function of a compact reverberant cavity, i.e., (a) $h(t)$ and (b) $|H(\omega)|$.

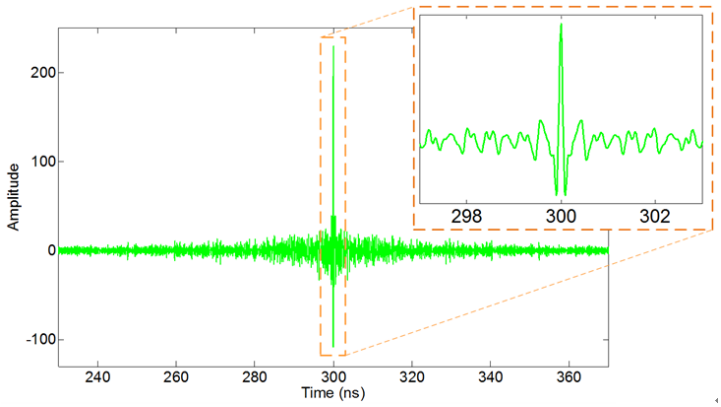

Figure 3. Time domain plot of the cavity output after TR, $y(t)$.

of the impulse response into the cavity. The output of the cavity after applying TR is

$$y(t) = h(t) * h(T - t) \tag{1}$$

where $*$ denotes convolution and T is the duration of the measured cavity impulse response. With the time-delay information reversed, $h(T-t)$ propagates inside the cavity following the same multipath ray trajectories, consequently removing the multipath delays and allowing the waves to focus at the output port to from a compressed short pulse at $t = T$. Fig. 3 shows $y(t)$ generated using $h(t)$ from Fig. 2(a). A short pulse is observed at $t = T = 300$ ns that closely resembles the original impulse (see inset of Fig. 2(a)) with time "sidelobes" which is an inherent feature of a TR reconstructed pulse arising from the non-focusing waves, which can be seen as leakage in pulse compression. These non-focusing waves are generated due to the omni-directionality of the cavity feeds. From a signal processing point of view $y(t)$ represents the autocorrelation of $h(t)$.

In the frequency domain, time-reversal corresponds to phase conjugation and the resulting output signal is represented as

$$Y(\omega) = H(\omega)H^*(\omega) = |H(\omega)|^2 e^{j\omega T}, \tag{2}$$

where the phase is completely canceled out since $e^{j\omega T}$ corresponds to the time shift. Fig. 4 presents the plots of the magnitude and phase (with $e^{j\omega T}$ term neglected) of $Y(\omega)$. Since $|H(\omega)|^2$ is real valued, i.e., the Fourier series coefficients are real, all frequencies add coherently at $t = T$ to form a short pulse. However, the non-uniform amplitude across the bandwidth (with peaks and nulls) gives rise to time sidelobes in $y(t)$.

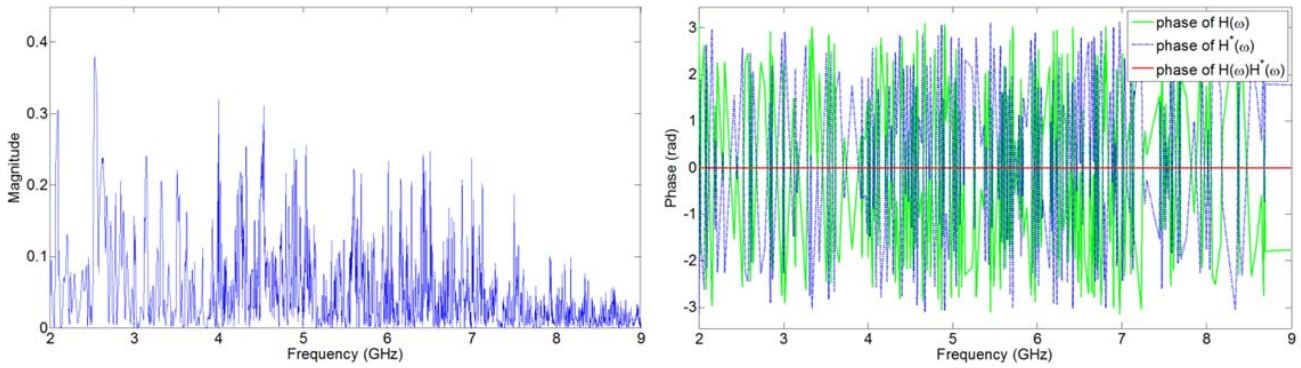

(a) (b)

Figure 4. Frequency domain plot of the cavity output after TR, $Y(\omega)$: (a) $|Y(\omega)|$ and (b) phase of $|Y(\omega)|$ without $e^{j\omega T}$ term (red) in comparison with phases of $H(\omega)$ (green) and $H^*_{ob}(\omega)$ (blue).

Now consider the peak gain (or compression gain), PG, defined as the ratio between the peaks of the output and input waveforms, that is,

$$PG = 10 \log \left[\left(\frac{\max\{|y(t)|\}}{M} \right)^2 \right], \tag{3}$$

where $M = \max\{|h(t-T)|\}$. Using Eq. (3), PG from the examples in Figs. 2 and 3 is calculated to be 3.5 dB, which is not a significant gain considering the input waveform duration and bandwidth. Although a compressed short pulse is generated at the output, the amplitude decay in the original $h(t)$ limits the maximum achievable peak amplitude of $y(t)$. In other words, the time-amplitude space is not fully utilized to maximize the input energy. One way to overcome this problem is to apply OBTR [11]. In OBTR, the amplitude of $h(t)$ is essentially quantized down to a single-bit (with sign) by setting the waveform amplitude to be either M or $-M$ around zero crossings, namely

$$h_{ob}(t) = \begin{cases} M, & \text{if} \quad h(t) \geq 0 \\ -M, & \text{if} \quad h(t) < 0 \end{cases}. \tag{4}$$

This allows a uniform amplitude across the whole waveform (Fig. 5), thereby maximizing the input energy without sacrificing much of the delay (phase) information essential for time-reversal reconstruction. The output of the cavity after applying OBTR is

$$y_{ob}(t) = h(t) * h_{ob}(T-t). \tag{5}$$

Figure 6 shows $y_{ob}(t)$ in comparison to $y(t)$, where a significant increase in peak amplitude is observed. By substituting $y_{ob}(t)$ into Eq. (3) the peak gain from OBTR, namely PG_{ob}, is calculated to be 17.4 dB. An overall increase in time sidelobes is observed in $y_{ob}(t)$, especially to the left of the reconstructed pulse, due to a flat higher amplitude in the one-bit waveform. Time sidelobes to the right of the pulse decay in the same manner as that in $y(t)$ as there is no input energy after $t = T$.

In the frequency domain, the output is represented as

$$Y_{ob}(\omega) = H(\omega) H^*_{ob}(\omega) e^{j\omega T}. \tag{6}$$

As shown in Fig. 7(a), the magnitude level of $Y_{ob}(\omega)$ is indeed significantly higher than that of $Y(\omega)$ in Fig. 4(a) due to higher energy content. Note that $Y_{ob}(\omega)$ does not have completely zero phase since the phases of $H_{ob}(\omega)$ and $H(\omega)$ are not exactly matched anymore (i.e., $H(\omega)H^*_{ob}(\omega) \neq |H(\omega)|^2$) due to the one-bit process. This none-zero phase results in some frequencies adding non-coherently, which explains the increase in time-sidelobes in the time-domain. However, the phase of $Y_{ob}(\omega)$ mostly revolves around zero, with many of the phase components remaining at zero especially at frequencies with high resonant peaks. This still allows for many of the frequencies to add coherently to form a high peak at $t = T$.

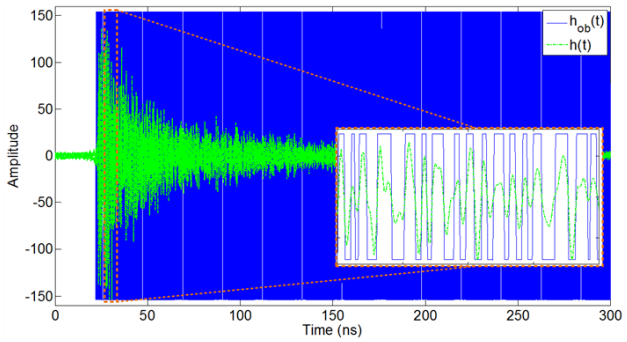

Figure 5. One-bit cavity impulse response, $h_{ob}(t)$, in comparison to the original impulse response $h(t)$.

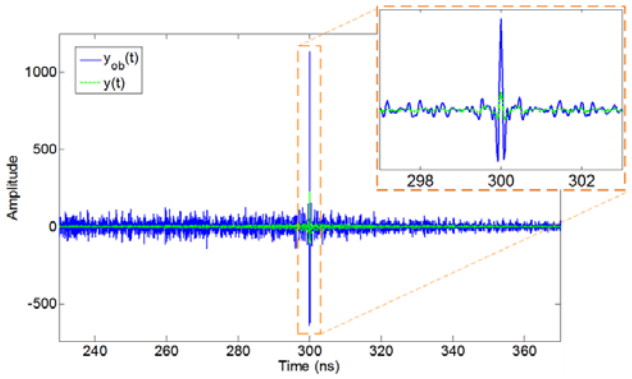

Figure 6. Time domain plot of the cavity output after OBTR, $y_{ob}(t)$ (blue) in comparison with the output after TR, $y(t)$ (green).

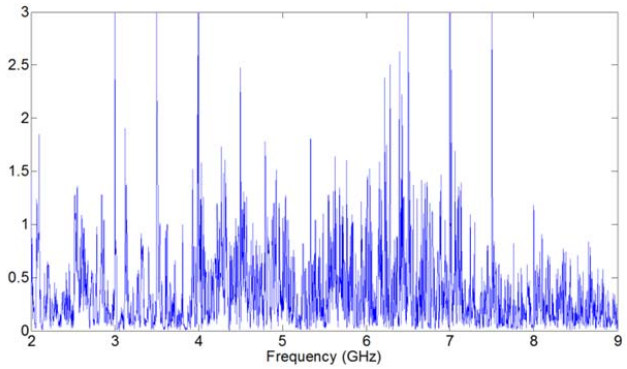

(a)

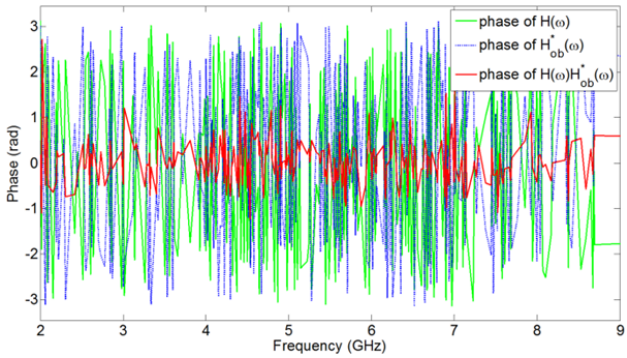

(b)

Figure 7. Frequency domain plot of cavity output $Y_{ob}(\omega)$ after OBTR: (a) $|Y_{ob}(\omega)|$ and (b) phase of $Y_{ob}(\omega)$ without $e^{j\omega T}$ term (red) in comparison with phases of $H(\omega)$ (green) and $H^*_{ob}(\omega)$ (blue).

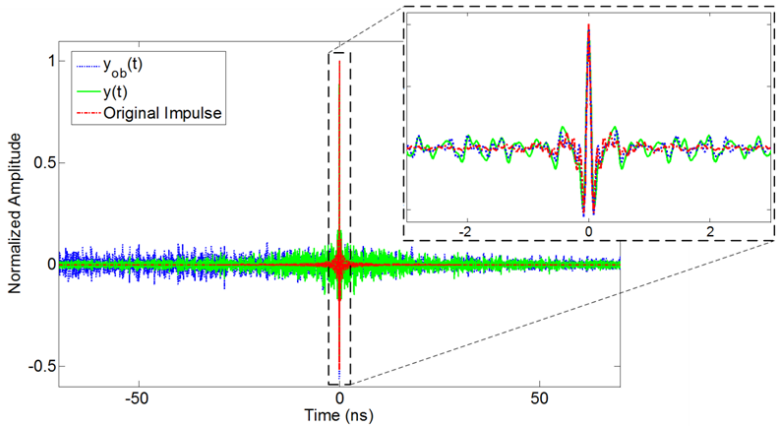

Figure 8. Normalized original impulse (red), TR output $y(t)$ (green), and OBTR output $y_{ob}(t)$ (blue).

To check the fidelity of the compressed pulse via OBTR, $y_{ob}(t)$ with normalized amplitude is plotted along with the original impulse and $y(t)$ (also normalized) in Fig. 8. Note that $y_{ob}(t)$ and $y(t)$ are time-shifted by T. In the figure, a short pulse closely resembling the original impulse is observed in $y_{ob}(t)$. Moreover, $y_{ob}(t)$ seems to have sidelobes with slightly lower peaks compared to $y(t)$, even though it

contains a larger number of time sidelobes. A good metric for pulse quality to use is the peak-to-leakage ratio, PLR, defined as the ratio of the peak of the compressed pulse to maximum time sidelobe amplitude:

$$PLR = 10\log\left[\left(\frac{\max_{t\in T}\{|y_{ob}(t)|\}}{\max_{t\in T-[t_i,t_f]}\{|y_{ob}(t)|\}}\right)^2\right], \tag{7}$$

where $[t_i, t_f]$ is the timewidth that bounds the compressed pulse. The PLR provides insight into the relative level of energy leakage due to time sidelobes during the pulse compression process. Using this definition, $y_{ob}(t)$ in Fig. 8 has a PLR of 18.1 dB whereas the PLR for $y(t)$ is 16.7 dB.

3. PULSE COMPRESSOR EXPERIMENT

3.1. Experiment Setup

We constructed an experimental pulse compressor consisting of a compact reverberant cavity, as shown in Fig. 9. The inner dimensions of the cavity are 0.58 m × 0.32 m × 0.04 m ($W \times D \times H$) with the corresponding volume of 0.0074 m^3. This cavity is a semi-2D cavity, where the waves reverberate only in the horizontal (broad) plane. In other words, the eigenmodes (resonances) are found only in the horizontal plane with no modal variation in the vertical plane. The cavity dimensions chosen here ensure an overmoded condition across the bandwidth of the impulse (2–9 GHz), i.e., the lowest eigenmode frequency is well below 2 GHz. An X-shaped scatterer is placed inside the cavity as a mode-mixer. Since the cavity consists of a complex propagation environment which is ray-chaotic, a slight change in the feed or mode-mixer position could result in completely different multipath trajectories between the input and output ports, producing different impulse responses which may influence the pulse compression performance. In this experiment we have varied the mode-mixer position by rotating it over 224 discrete angles and studied the effect on pulse compression.

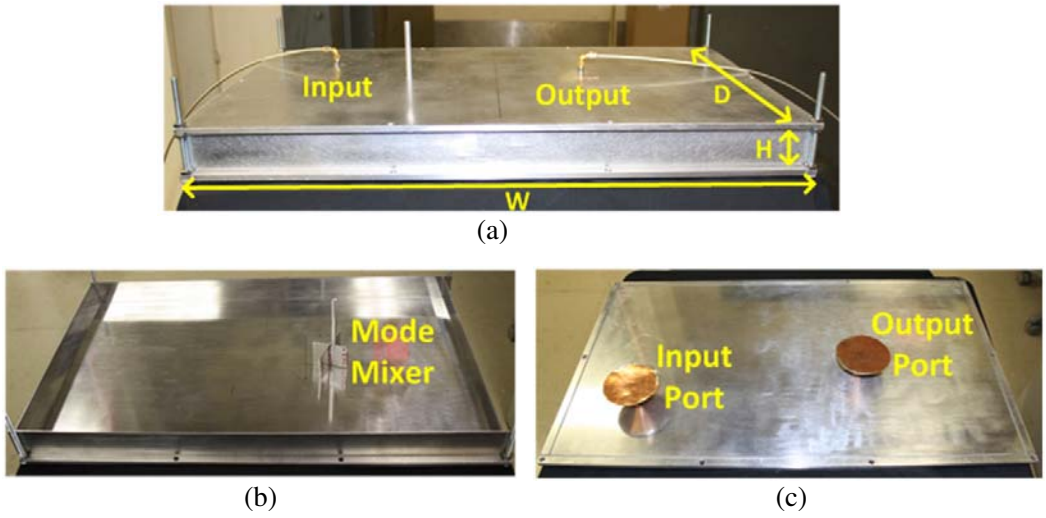

Figure 9. The compact reverberant cavity used in the pulse compressor experiment: (a) Overall exterior view (W, H and D correspond to the inner dimensions), (b) cavity with the top plate off, showing the inside, and (c) the interior part of the top plate, showing the input and output ports.

The experiment setup consisted of an arbitrary waveform generator (Tektronix AWG70002) as a waveform source connected to the cavity input and a digital oscilloscope (Tektronix DPO72004) to capture the cavity output waveforms (Fig. 10). The experimental procedure generally followed the diagram in Fig. 1, where an impulse (as shown in Fig. 2(a)) is first transmitted into the cavity to measure and record $h(t)$ for a time duration of T, which is then processed for OBTR. $h_{ob}(T-t)$ is then

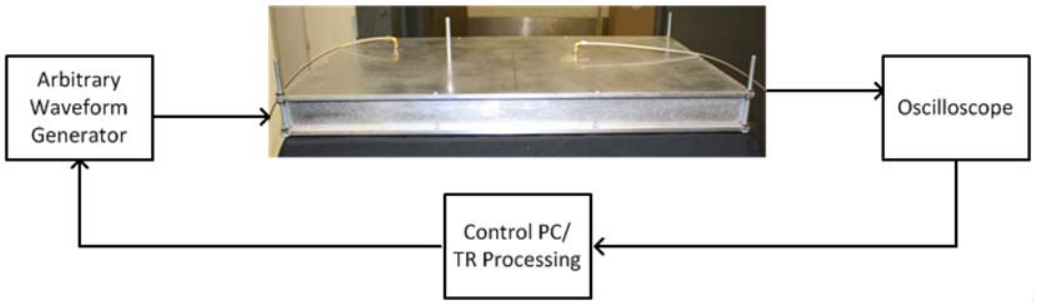

Figure 10. Pulse compression experiment setup.

transmitted back into the cavity to produce a compressed ultrashort pulse $y_{ob}(t)$. The sampling rate of the arbitrary waveform generator was set at 25 Gs/s, which was sufficient to generate a 130 ps impulse as at least three samples are contained within that pulsewidth. The scope sampling rate was also set at 25 GS/s to maintain the same signal bandwidth in $h(t)$. If $h(t)$ is recorded at a slower sampling rate, then the signal bandwidth would be limited, stretching the output pulse to be wider than the original impulse with a lower peak amplitude, thereby reducing the peak gain.

In every measurement the input waveform $h_{ob}(T-t)$ has a duration T of 300 ns. A power amplifier was not used in this experiment. Therefore the input amplitude remained at 0.25 V, which was the maximum output level of the arbitrary waveform generator. Depending on the desired peak power level in a practical scenario, a power amplifier with an appropriate bandwidth can be added. The cavity feeds also need to be designed properly according to the output power requirement.

3.2. Results and Discussion

Figure 11 shows $y_{ob}(t)$ measured with the mode-mixer position that produced the maximum compression gain (PG) of 19.6 dB, where a short compressed pulse resembling the original impulse is observed with a peak amplitude of 2.4 V. The compressed pulse in this case also closely resembles the original impulse with time sidelobes generated due to leakage similar to that from Fig. 6. While all of the measured output waveforms share the same features, i.e., compressed short pulse with time sidelobes, the peak amplitude level varies and therefore the PG values. In Fig. 12, the PG values obtained from all 224 mode-mixer positions are plotted, where a few points above 19 dB are observed as well as a few points below 15 dB. The minimum gain obtained from this set of measurements is 14.6 dB. The majority of the PG values seem to be around 17 dB, which is also the average PG value.

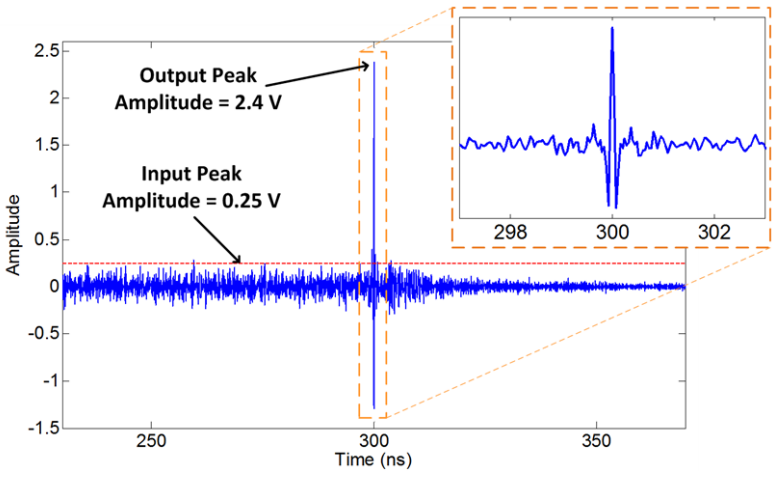

Figure 11. Measured output after OBTR pulse compression showing 19.6 dB of peak gain.

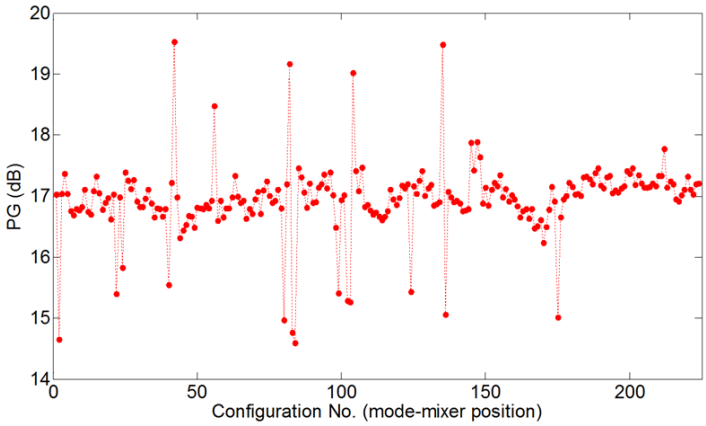

Figure 12. Compression gain obtained from various different configurations by varying the mode-mixed position.

This experiment shows that the cavity configuration influences the achievable compression gain. Thus it may be necessary to carry out an "optimization" in order to determine the configuration that produces the maximum gain for a given reverberant cavity. However, even without this optimization, the statistics show that there is an expected PG value (17 dB in this case) which is still significant. Therefore, determining whether to optimize the cavity would depend on the application and operation of the pulse compressor.

Compression efficiency is also an important parameter to discuss as it is a measure of energy conversion from input to output. Here we calculate the compression efficiency to be the ratio of the energies in the output to input signal. The compression efficiency of our experimental system is less than 10%. This number is significantly lower than the reported efficiency of other pulse compression systems typically ranging between 40–60% [3–8]. The low efficiency of our compressor is primarily due to the loss in the cavity, which is evident from the transfer function plotted in Fig. 2(b), where most of the eigenmodes peaks are below 0.5 (−6 dB). For a lossless cavity, the eigenmodes peaks should be 1 (0 dB), which would result in a significantly higher efficiency. A large portion of the cavity loss is due to the feed ports. Hence, a design improvement in the feed ports would be necessary in order to increase the compression efficiency. Another way to further increase the efficiency is to optimize the input waveform duration T such that T roughly corresponds to the time at which most amplitude has decayed in $h(t)$. Increasing the efficiency would also result in higher peak gain.

4. CONCLUSION

In this paper, we propose a passive pulse compressor capable of generating ultrashort microwave pulses based on a compact reverberant cavity. One-bit time-reversal is applied to create a long duration flat-amplitude input waveform that contains the inverse phase distortion of the cavity, so as to create a compressed high peak ultrashort pulse as a result of phase cancellation due to time-reversal. We have built and demonstrated an experimental pulse compressor that can generate a 130 ps output pulse with up to 19 dB of peak gain (with 17 dB of expected gain value from statistics). By designing and optimizing the cavity for a desired pulse width and peak power level, this pulse compressor could be used in various applications requiring high peak ultrashort pulses such as directed energy, high resolution radar, biomedical and short pulse wireless power transfer.

REFERENCES

1. Gaponov-Grekhov, A. V. and V. L. Granastein, *Applications of High-power Microwave*, Artech House, Norwood, MA, 1994.
2. Schamiloglu, E., "High power microwave sources and applications," *2004 IEEE MTT-S Digest*, 1001–1004, 2004.

3. Tantawi, S. G., R. D. Ruth, A. E. Vlieks, and M. Zolotorev, "Active high-power RF pulse compression using optically switched resonant delay lines," *IEEE Trans. Microw. Theory Tech.*, Vol. 45, No. 8, 1486–1492, 1997.
4. Farr, E. G., L. H. Bowen, W. D. Prather, and C. E. Baum, "Microwave pulse compression experiments at low and high power," *Circuit and Electromagnetic System Design Notes*, No. 63, 2010.
5. Vikharev, A. L., A. M. Gorbachev, O. A. Ivanov, V. A. Isaev, S. V. Kuzikov, M. A. Lobaev, J. L. Hirshfield, S. H. Gold, and A. K. Kinkead, "High power active X-band pulse compressor using plasma switches," *Phys. Rev. Spec. Top. Accel. Beams*, Vol. 12, 062003, 2009.
6. Thirios, E. C., D. I. Kaklamani, and N. K. Uzunoglu, "Pulse compression using a periodically dielectric loaded dispersive waveguide," *Progress In Electromagnetics Research*, Vol. 48, 301–333, 2004.
7. Burt, G., S. V. Samsonov, A. D. R. Phelps, V. L. Bratman, K. Ronald, G. G. Denisov, W. He, A. R. Young, A. W. Cross, and I. V. Konoplev, "Microwave pulse compression using a helically corrugated waveguide," *IEEE Trans. Plasma Sci.*, Vol. 33, No. 2, 661–667, Apr. 2005.
8. McStravick, M., S. V. Samsonov, K. Ronald, S. V. Mishakin, W. He, G. G. Denisov, C. G. Whyte, V. L. Bratman, A. W. Cross, A. R. Young, and P. MacInnes, "Experimental results on microwavepulse compression using helically corrugated waveguide," *J. Appl. Phys.*, Vol. 108, 054908, 2010.
9. Daniels, D., "Applications of impulse radar technology," *Radar Systems (RADAR 97)*, 667–672, Oct. 1997.
10. Lalande, M., J.-C. Diot, S. Vauchamp, J. Andrieu, V. Bertrand, B. Beillard, B. Vergne, V. Couderc, A. Barthelemy, D. Gontier, R. Guillerey, and M. Brishoual, "An ultra wideband impulse optoelectronic radar: RUGBI," *Progress In Electromagnetics Research B*, Vol. 11, 205–222, 2009.
11. Yang, C.-L., Y.-L. Yang, and C.-C. Lo, "Subnanosecond pulse generators for impulsive wireless power transmission and reception," *IEEE Trans. Circuits Syst. II, Exp. Briefs*, Vol. 58, No. 12, 817–821, Dec. 2011.
12. Giri, D. V., *High-power Electromagnetic Radiators: Nonlethal Weapons and Other Applications*, Harvard University Press, Cambridge, MA, 2004.
13. Converse, M., E. J. Bond, B. D. van Veen, and S. C. Hagness, "A computational study of ultra-wideband versus narrowband microwave hyperthermia for breast cancer treatment," *IEEE Trans. Microw. Theory Tech.*, Vol. 54, No. 5, 2169–2180, May 2006.
14. Derode, A., Tourin and A. Fink, "Ultrasonic pulse compression with one-bit time reversal through multiple scattering," *J. Appl. Phys.*, Vol. 85, No. 9, 6343–6352, May 1999.
15. Montaldo, G., P. Roux, A. Derode, C. Negreira, and M. Fink, "Generation of very high pressure pulses with 1-bit time reversal in a solid waveguide," *J. Acoust. Soc. Am.*, Vol. 110, No. 6, 2849–2857, Dec. 2001.
16. Davy, M., J. de Rosny, and M. Fink, "Focusing and amplification of electromagnetic waves by time reversal in a leaky reverberation chamber," *C. R. Phys.*, Vol. 11, 37–43, Feb. 2010.
17. Nguyen, H. T., "On the performance of one bit time reversal for multi-user wireless communications," *Int. Symposium on Wireless Comm. Systems (ISWCS 2007)*, 672–676, Oct. 2007.
18. Lerosey, G., J. de Rosny, A. Tourin, A. Derode, and M. Fink, "Time reversal of wideband microwaves," *Appl. Phys. Lett.*, Vol. 88, 154101, 2006.
19. Fink, M., D. Cassereau, A. Derode, C. Prada, P. Roux, M. Tanter, J. L. Thomas, and F. Wu, "Time reversed acoustics," *Rep. Prog. Phys.*, Vol. 63, No. 12, 1933–1995, 2000.